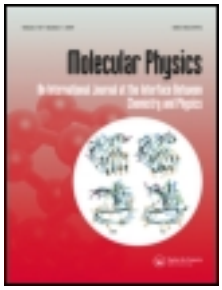

Molecular Physics: An International Journal at the Interface Between Chemistry and Physics
Publication details, including instructions for authors and subscription information:
http://www.tandfonline.com/loi/tmph20

Electron transfer processes of atomic and molecular doubly charged ions: information from beam experiments

Zdenek Herman [a]
[a] V. Čermák Laboratory , J. Heyrovský Institute of Physical Chemistry, Academy of Sciences of the Czech Republic , Prague , Czech Republic
Published online: 14 Jun 2013.

To cite this article: Zdenek Herman (2013): Electron transfer processes of atomic and molecular doubly charged ions: information from beam experiments, Molecular Physics: An International Journal at the Interface Between Chemistry and Physics, DOI:10.1080/00268976.2013.771804

To link to this article: http://dx.doi.org/10.1080/00268976.2013.771804

Molecular Physics, 2013
http://dx.doi.org/10.1080/00268976.2013.771804

Electron transfer processes of atomic and molecular doubly charged ions: information from beam experiments

Zdenek Herman*

V. Čermák Laboratory, J. Heyrovský Institute of Physical Chemistry, Academy of Sciences of the Czech Republic, Prague 8, Czech Republic

(*Received 14 December 2012; final version received 26 January 2013*)

Single-electron transfer reactions in collisions of atomic and molecular doubly charged ions, with atoms and molecules, were investigated in a series of crossed-beam scattering, translational spectroscopy and product luminescence experiments. Investigation of a series of atomic dication-atom electron transfer at collision energies of 0.1–10 eV provided data on differential and relative total cross sections of state-to-state processes. Populations of electronic and vibrational states and rotational temperatures of molecular product ions were obtained from studies of non-dissociative electron transfer in systems containing simple molecular dications and/or molecular targets. The product electronic states populated with highest probability were those for which the translational energy release was 3–5 eV, indicating that the 'reaction window' concept, based on the Landau–Zener formalism, is applicable also to molecular systems. Population of the vibrational states of the molecular products could be described by Franck–Condon factors of the vertical transitions between the reactant and product states, especially at higher (keV) collision energies. Rotational temperature of the product molecular cations was found to be surprisingly low, mostly 400–500 K, practically the temperature of the ion source.

Keywords: doubly charged ions; electron transfer processes; beam experiments

1. Introduction

The physics and chemistry of multiply charged ions have been steadily growing up through the past four decades. Motivation for the studies of structure of multiply charged particles and their interaction in collisions with other particles stems from the realisation of their importance in many areas of physics – from plasma, discharge and fusion physics to astrophysics. Naturally, the first objective was to study the properties and behaviour of atomic multiply charged ions. Though the existence of molecular multiply charged ions has been known since the 1920s [1,2], detailed information – both experimental and theoretical – on their stability, electronic structure, spectroscopic properties and energetics comes mostly from the 1980s and 1990s.

Among the interaction of multiply charged ions with other particles, electron transfer (charge transfer, electron exchange) was the process studied most often, especially the process involving transfer of one electron:

$$A^{n+} + B \rightarrow A^{(n-1)+} + B^{+}$$

Processes of this type were investigated over a wide range of velocities of charged projectiles, and three dynamical regions of velocity v were established, the low velocity ($v \ll v_0$ with the atomic unit $v_0 = 2.19 \times 10^8$ cm s^{-1}), intermediate ($v \sim v_0$) and high ($v \gg v_0$). Total cross sections of processes and their dependence on the energy of projectiles were among the first targets of the studies. Later on, state-selective processes were investigated; in particular processes in which electronic state of the product cations was identified using, in most cases, the translation energy spectroscopy method. Several excellent reviews were published over the years that quote also the earlier reviews and books on the subject [3,4].

This communication is a summary of the activity of the Prague research group and several collaborating laboratories over a longer period of time, with inclusion of work of others whenever the subject requires it. The research concerned studies of collision processes of atomic and molecular doubly charged ions (dications) in the low velocity region, to incident energies of the order of several keV ($v \sim 10^7$ cm s^{-1}) and, in particular, of several eV ($v \sim 10^5$ cm s^{-1}). The aim of this research was to obtain new data to enable a detailed description of the processes of electron transfer [5,6] and chemical reactions [7,8] of atomic and molecular dications by obtaining information in particular on

(1) dynamics of electron transfer processes;
(2) differential cross section (angular distribution) of products;

*Email: zdenek.herman@jh-inst.cas.cz

(3) partitioning of various forms of energy in molecular reaction products;
(4) relative total cross sections for different state selected processes.

Further scattering studies concerned chemical reactions of dications and mutual relations between electron transfer processes and chemical reactions of these species [7,8].

2. Experimental methods

The results reviewed in this paper were obtained mostly by three experimental methods, namely, the crossed-beam scattering method, the translational spectroscopy method, and the product luminescence method. In all these methods, the objective is analysis of the properties of product ions. In the beam scattering method it is the analysis of translational energy (velocity) and angular distribution of the product ions, in translational spectroscopy it is the translational energy analysis of the product ions, and in the luminescence method it is the spectroscopic analysis of the light emitted by the reaction products.

2.1. The crossed-beam scattering method

Most of the data on dication-neutral reactions in the eV collision energy region reported here were obtained in crossed-beam scattering experiments using the Prague crossed-beam apparatus EVA II. The performance and application of the machine to this type of scattering experiment have been described previously [7,8]. In the experiments of this type, a beam of dications was produced by electron ionisation of neutral molecules in a low-pressure ion source. The ions were extracted, mass analysed, and decelerated by a multi-element lens to the required laboratory energy. The dication beam was crossed at right angle with a collimated beam of neutral target molecules emerging from a multi-channel jet. The ion beam had an angular and energy spread of 1° and 0.4 eV (full width at half-maximum, FWHM), respectively; the collimated neutral beam had an angular spread of 6° (FWHM) and thermal energy distribution at 300 K. Reactant and product ions passed through a detection slit into a stopping potential energy analyser. They were then accelerated and focused into the detection mass spectrometer, mass analysed, and detected with the use of an electron multiplier. Angular distributions were obtained by rotating the two beams about the scattering centre. Modulation of the neutral beam and phase-sensitive detection of the ion products were used to remove background scattering effects. Laboratory angular distributions were repeatedly recorded and the results were averaged. Energy profiles of the product ions were recorded several times at each of a series of laboratory scattering angles, the results were averaged, and the laboratory energy distributions were converted to velocity distributions. The laboratory angular and velocity distributions were used to construct scattering diagrams of the investigated product ions. The contours in the scattering diagrams refer to the Cartesian probability distribution [8], normalised to the maximum in a particular scattering diagram. Centre-of-mass (CM) angular distributions (relative differential cross sections), $P(\theta_{CM})$ vs. θ_{CM}, and relative translational energy distributions, $P(T')$ vs. T', of the product ions were obtained by appropriate integration of the scattering diagrams [8,9] (the designation T' is used for relative translational energy of products and T for relative translational energy of reactants).

Some of the crossed-beam data on electron transfer between He^{2+} and molecular targets [10,11] were obtained on the Göttingen high-resolution apparatus used earlier in studies of proton and deuteron collisions with polyatomic molecules [12]. The beam of He^{2+} was produced in a Colutron gas-discharge source, extracted, mass selected by a Wien filter and energy selected by a hemispherical electrostatic selector. The energy and angular width of the reactant ion beam was better than 100 meV and 1.5°, respectively. The He^{2+} beam was crossed at right angle by a skimmed nozzle beam of neutral target molecules. The product He^{+} ions were analysed by a system consisting of a focusing lens, another hemispherical electrostatic energy analyser and a focusing lens system, and detected on an electron multiplier. The analyser system could be rotated about the axis of the target beam in the plane of the projectile beam.

2.2. The translational spectroscopy method

Translational energy spectroscopy was used to obtain data on electron transfer products of dication-neutral product at keV energies. In the method, translational energy of products is measured along the direction of the reactant dication beam. The experiments were conducted with the ZAB-2F reversed-geometry double-focusing mass spectrometer of the University College of Swansea [13] and the experimental procedure was described elsewhere [14]. The dications, produced by electron ionisation in a Nier-type ion source, extracted and accelerated to 6 keV, and mass selected by a sector magnet, entered a collision cell with the target gas at a pressure of about 0.2 Pa. Translational energy spectra were obtained under high-resolution conditions by scanning the voltage of the cylindrical electrostatic analyser.

2.3. The product luminescence method

Results on product ion luminescence were obtained on the beam-luminescence apparatus of the Max Planck Institute for Fluid Research, Göttingen, in cooperation with the research group of Ch. Ottinger. The apparatus [15,16] consisted of a special ion source, a mass selecting magnet, a collision cell, light collection optics imaging the interaction region onto the entrance slit of a spectrograph and

a position-sensitive detector. A special, low-pressure ion source produced molecular dications by ionisation using 300 eV electrons. The ions were extracted through an orifice, accelerated to 2 keV, mass analysed by a magnetic sector and decelerated down to the desired energy with a simple immersion lens in front of the collision chamber. Luminescence of the reaction products in the collision cell was observed at right angle to the ion beam. The emission passed through a quartz window, and was focused by a spherical mirror onto the entrance slit of a grating spectrometer (McPherson 218) equipped with a stepping motor. A position-sensitive photomultiplier and digital processing equipment was used to detect and process the signals. Spectra were obtained by repetitive scanning over a pre-selected wavelength range.

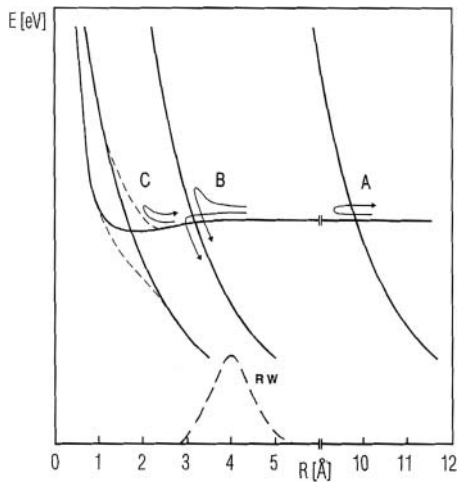

Figure 1. Schematics of potential energy curves for the electron transfer reaction – atomic dication-atom to atomic cations. For details see text: only case B leads to electron transfer of a considerable cross section within the 'reaction window' (RW).

3. Results and discussion

3.1. Models: the Landau–Zener formalism

Several models have been developed [3] to describe electron transfer between an atomic doubly charged ion and a neutral atomic target, a specific variant of reaction (1). The interaction potentials involved are rather simple. The interaction between the reactants is determined primarily by the ion-induced attraction between the dication and the neutral particle, combined with repulsion at small inter-nuclear separations. The interaction between the products is mainly characterised by Coulomb repulsion between two particles of the same charge. The reaction-product interaction terms usually cross under and acute angle and the crossings are well localised. The Landau–Zener (LZ) formalism can then be applied in most cases to describe the transition probability. The LZ approach describes well the total cross section and its dependence on collision energy [3,4,17], and it was used successfully to characterise the differential cross section [18]. An important conclusion of this approach is that the total cross section passes through a maximum, related to the position of the crossing point and the collision energy (Figure 1): if the crossing occurs at very large inter-nuclear separations, where the interaction and the transition probability are very small, the collision system tends to stay on the incoming potential energy curve (A in Figure 1); if the crossing occurs at very small inter-nuclear separations, where the interaction is large and the single-passage transition probability is close to unity, the terms split adiabatically, and the system approaches and departs on the reactant potential energy curve (C); only if the crossing occurs at intermediate inter-nuclear separations, where the transition probability is about 0.5 or so, there is a finite chance that the collision system may depart on the product potential energy curve (B). As a consequence, the exothermicity of the electron transfer process has to fit into a 'reaction window' for the process to occur efficiently (RW in Figure 1, the dashed line indicates schematically the cross section). Numerous experimental verifications of the reaction window concept have been obtained, though deviations from the applications of the simple LZ model are known too.

3.2. Atomic systems

The first system studied in our scattering experiments was the electron transfer process between an atomic dication and a neutral atom [19]:

$$Ar^{2+}(^3P, ^1D, ^1S) + He(^1S) \rightarrow Ar^{+}(^2P) + He^{+}(^2S) \quad (1)$$

(references to fine structure states, not resolved in the experiments, are omitted). The reactant beam, formed by electron ionisation, contained, besides the ground-state $Ar^{2+}(^3P)$ dications, metastable excited states $Ar^{2+}(^1D)$ and $Ar^{2+}(^1S)$ as well. Therefore, there were three possible entrance channels, characterised by ion-induced dipole interaction between the dication and the neutral at larger inter-nuclear separations and repulsion at small inter-nuclear separations, and one exit channel, characterised essentially by Coulomb repulsion between the two singly charged products. The exothermicities of these processes were 3.00, 4.74 and 7.12 eV for the reactant dication states (^3P), (^1D) and (^1S), respectively. The scattering diagrams of the product Ar^{+} at collision energies of 0.53 and 1.62 eV are shown in Figure 2. The intensity ridges clearly show formation of Ar^{+} in reactions of $Ar^{2+}(^3P)$ and $Ar^{2+}(^1D)$, while the reaction of $Ar^{2+}(^1S)$ appears to contribute only negligibly. The structures in the scattering diagram could be de-convoluted to extract data on relative differential cross

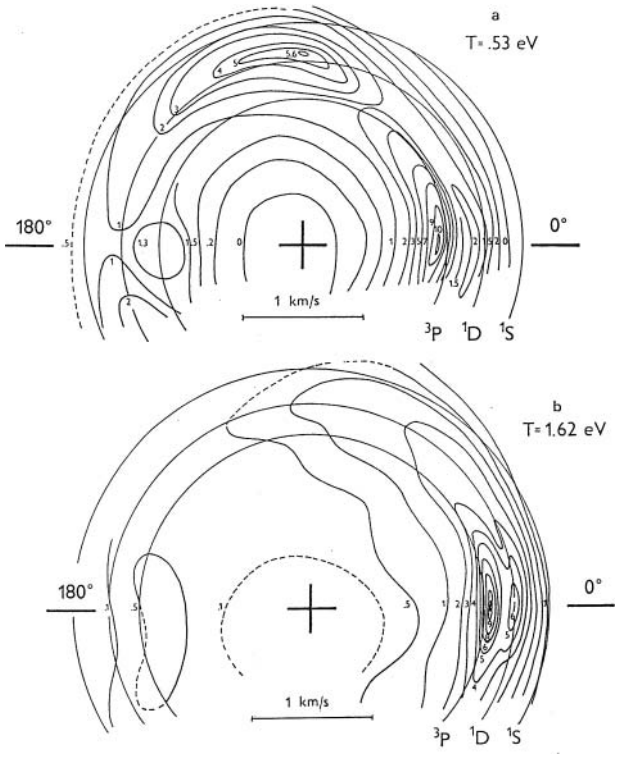

Figure 2. Contour scattering diagrams of Ar^+ from reaction (1) at collision energies of 0.53 and 1.62 eV: circles represent loci of CM velocities as expected from exothermicities of processes with Ar^{2+} in different electronic states; crosses mark the position of the tip of the CM velocity vector; relative velocity is directed along the 180°–0° axis.

sections (CM angular distributions) of the respective state-to-state processes (Figure 2).

To understand better the shape of the differential cross section, a simple quasi-classical model was developed and the differential cross section of the state-to-state process

$$Ar^{2+}(^3P) + He(^1S) \rightarrow Ar^+(^2P) + He^+(^2S) \qquad (2)$$

was calculated [18]. The two-level model assumed that the interaction between the reactants was determined – as mentioned above – by the ion-induced dipole interaction potential combined by a strong repulsion at small separations (represented by a steep wall) and for the product by Coulomb repulsion potential between two singly charged ions. The analysis of the quasi-molecular terms showed that the leading reactant–product interaction terms were the $^3\Pi$ terms. Coupling of the diabatic terms was calculated using the asymptotic method. The LZ model was used to determine the respective transition probabilities, assumed to be localised in the crossing points between the reactant–product potential terms. Two trajectories at each impact parameter b, reflecting the movement of particles under the influence of different potential on the way in and out,

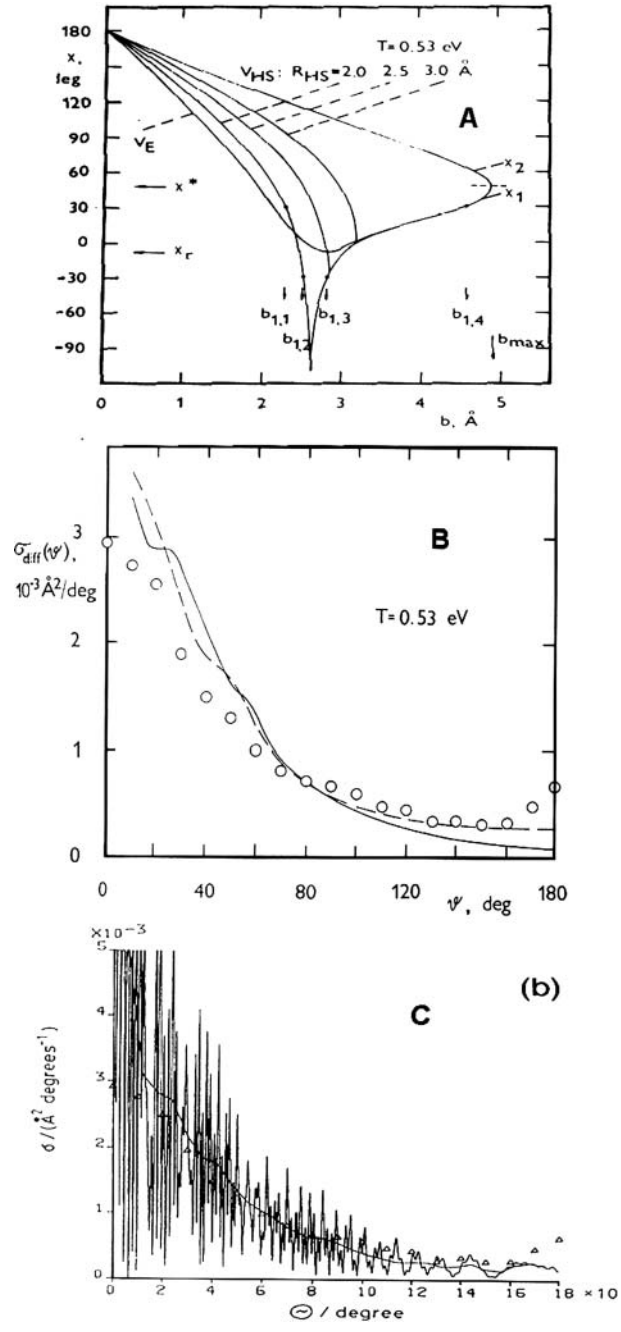

Figure 3. Analysis of the differential cross section of state-to-state reaction (2): A – deflection functions used in the semi-classical model; B – results of the semi-classical model calculations: open points – experimental data, dashed and solid line – results using different deflection functions; C – results of quantum chemical calculations [20]: triangles – experimental data, smooth solid line – data averaged over experiment resolution.

contributed to the cross section. Consequently, the calculated deflection function had two branches smoothly connecting in the vicinity of b_{max} (Figure 3A). The quasi-classical differential cross section, calculated with the use of these simple potentials, described correctly

the shape of the differential cross section, derived from the above-mentioned experiments (Figure 3B), in particular the prominent forward peaking of the product Ar^+.

The differential cross section of reaction (2) was subjected to another theoretical study [20] in which the two lowest $^3\Pi$ potential energy surfaces were calculated by the *ab initio* configuration interaction procedure using a large basis set, transformed to diabatic potentials, and the total and differential cross sections were calculated using the quantum mechanical close coupling method. A comparison with the experimental differential cross section (Figure 3C) turned out to be good, after the calculated results were averaged over the CM angular resolution of the experiment ($\Delta\theta = 12^\circ$).

In the above-mentioned experiments, the spin–orbit states of the product could not be resolved. To answer the question about the relative population of spin–orbit states in a simple atomic dication–atomic neutral electron transfer process, reaction (3) was investigated in the scattering experiments [21]:

$$Hg^{2+}(^1S) + Kr(^1S) \rightarrow Hg^+(^2S) + Kr^+(^2P_{3/2}) \qquad \Delta_R H = -4.77 \text{ eV} \tag{3a}$$

$$Hg^{2+}(^1S) + Kr(^1S) \rightarrow Hg^+(^2S) + Kr^+(^2P_{1/2}) \qquad \Delta_R H = -4.12 \text{ eV} \tag{3b}$$

Figure 4 shows scattering diagrams of Hg^+ formed in this reaction. The intensity ridges of processes leading to different spin–orbit states can be clearly resolved. Figure 4 gives also the product relative translational energy distributions, $P(T')$ vs. T' (T' is relative translational energy of the products). De-convoluted areas under the curves give the ratio of total cross sections, $\sigma(3/2)/\sigma(1/2)$. For collision energies of 0.92, 1.16, 1.46 and 2.71 eV, this ratio was 1.2, 1.5, 1.4 and 0.8, respectively, i.e. on average about 1.2, which is somewhat smaller than the statistical ratio of forming the spin–orbit states of Kr^+ upon ionisation.

A similar result was obtained in studies of the reaction Kr^{2+} + He [22]. In this system, the reaction window concept favoured the reactions of the metastable $Kr^{2+}(^1S)$ (though statistically, little abundant in the beam)

$$Kr^{2+}(^1S) + He(^1S) \rightarrow Kr^+(^2P_{3/2}) + He^+(^2S_{1/2}) \qquad \Delta_R H = -4.07 \text{ eV} \tag{4a}$$

$$Kr^{2+}(^1S) + He(^1S) \rightarrow Kr^+(^2P_{1/2}) + He^+(^2S_{1/2}) \qquad \Delta_R H = -3.42 \text{ eV} \tag{4b}$$

over the reactions of $Kr^{2+}(^1D)$ of exothermicities 1.79 and 1.13 eV, respectively (reactions of the ground-state $Kr^{2+}(^3P)$ are endothermic). The ratio $\sigma(3/2)/\sigma(1/2)$ was

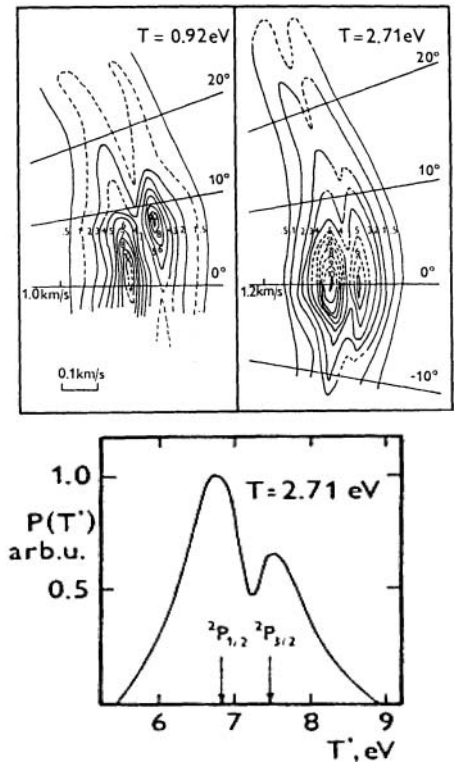

Figure 4. Scattering diagrams of Hg^+ (upper part) and relative translational energy distribution, $P(T')$–T' (lower part), of products of reaction (3a,b); T is relative translational energy of the reactants, T' is relative translational energy of the products. In the scattering diagrams, the maximum to the left is due to $Kr^+(^2P_{1/2})$ formation [reaction (3b)], the maximum to the right is due to $Kr^+(^2P_{3/2})$ formation [reaction (3a)].

about 1.0 at collision energies of 0.31 and 0.5 eV, respectively [22].

The scattering study [23] of the reaction

$$N^{2+}(^2P) + He\ (^1S) \rightarrow N^+(^3P, ^1D) + He^+(^2S) \tag{5}$$

was motivated by the effort to determine the ratio of the two electronic states of the product N^+, the ground-state $N^+(^3P)$ and the excited state $N^+(^1D)$. The reaction is of astrophysical interest because of its possible importance as a source of the metastable $N^+(^1D)$ in cold plasma nova shells. Data at collision energies above 100 eV showed strong preference for formation of the ground state, while theoretical calculations [24] at low energies indicated increased formation of the metastable state. The ratio $\sigma_{tot}(^1D)/\sigma_{tot}(^2P)$ was derived from the scattering diagrams obtained over the collision energy range, 5–12 eV. The ratio increased strongly with decreasing collision energy (Figure 5) and reached unity at about 5 eV. Semi-empirical calculations (dashed curve in Figure 5) using the LZ model fitted well this increase.

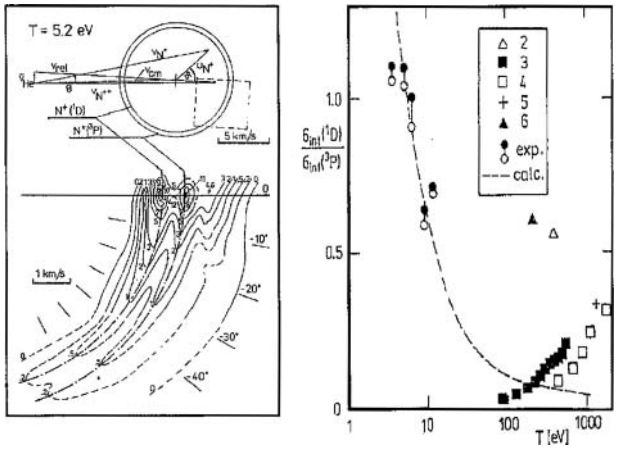

Figure 5. Scattering diagram of N^+ from reaction (5) (left) and ratio of total cross sections, $\sigma_{tot}(^1D)/\sigma_{tot}(^2P)$ (here designated σ_{int}), in dependence on collision energy T. Solid and open points – own experimental results; dashed line – own calculations; squares and triangles – high energy data from other sources (see text and [23]).

3.2.1. *Conclusions: atomic systems*

Scattering studies of the simple collision systems (atomic dication-atom)

(1) confirmed the applicability of the LZ formalism and the reaction window concept to estimate the population of electronic states of the reaction products;
(2) showed the prevailing forward scattering of the reaction products, and provided data on the differential cross sections, confirmed both by quasiclassical and quantum chemical calculations;
(3) made it possible to determine state-selected relative differential and total cross sections.

3.3. Molecular systems

In electron transfer collisions of dications involving molecular systems (molecular dication-atom, atomic dication-molecule, molecular dication-molecule), in addition to the question of population of the electronic states of the products, the question of population of the internal states of the molecular product cation formed, becomes important. In translational energy experiments this requires sufficient energy resolution so that both electronic and vibrational states of the product ion could be resolved by translation energy measurements and populations of the internal states determined. This can be achieved only for the simplest systems, and the problem becomes increasingly difficult if many internal states are populated (molecular dication-molecule systems). A combination of data from translational energy measurements and spectroscopy experiments (product luminescence) then becomes very important.

3.3.1. *Atomic dication-molecule*

Population of internal states of the molecular product ion formed from a neutral molecule was investigated by measuring the translational energy distribution of the atomic cation formed from the dication. Reactions of single-electron non-dissociative electron transfer of the dication He^{2+} with simple molecules NO [10], NH_3 and H_2S [11] were studied using the high-resolution Göttingen machine [12] at the incident energy of He^{2+} of 70 eV. The dication He^{2+} has very high recombination energy to the He^+ ground state (79.0 eV), and single-electron transfer giving the ground-state $He^+(^2S)$ would be out of the reaction window, presumably leading to a variety of dissociative processes. However, using a target molecule with the ionisation energy of about 10 eV or lower gave a chance that the reaction window concept would channel the electron transfer collision mostly to the excited state of $He^{+*}(^2P)$ (65.4 eV above the ground state), leaving about 4.5–3.5 eV for the exothermicity of the process, well within the reaction window. This turned out indeed to be the case.

The first reaction studied [10] was

$$He^{2+} + NO(^2\Pi) \rightarrow He^{+*}(^2P) + NO^+(^1\Sigma^+; v') \qquad (6)$$

The reaction is exothermic by 4.34 eV. Figure 6 shows translational energy distributions of the product He^+ at several scattering angles. The positions of the peaks corresponded well to the known vibrational spacing of $NO^+(^1\Sigma^+)$. The figure gives the relative population of the vibrational states derived from the spectra for a series of scattering angles (Figure 6d). The solid line indicates the population of vibrational states of $NO^+(^1\Sigma^+)$ as derived from photoelectron spectroscopy and theoretical calculations [25]. The population of NO^+ states from reaction (6) is very close to the Franck–Condon transition factors, with a slightly increased population of the levels of $v = 0$ and $v = 1$, if the populations were arbitrarily normalised to $v = 2$. No appreciable dependence on the scattering angle can be observed.

In another study of this series, reaction

$$He^{2+} + NH_3(^1A_1) \rightarrow He^{+*}(^2P) + NH_3^+(^2A_1; v^+) \qquad (7)$$

was investigated in an analogous way [11]. The translational energy spectrum of He^+ is shown in Figure 7, at the scattering angles of 0°, 1° and 2°. The vibrational spacing in $NH_3{}^+$ is smaller than that in NO^+, and thus, the peaks are not well resolved, but a simulation procedure could be used to provide the respective population of the vibrational states for several scattering angles. The result is shown in Figure 7, together with the vibrational spacing of the $\nu_2{}^+$ bending mode in $NH_3{}^+$ and the respective population of the transitions as known from photoelectron spectroscopy [26]. The populations reflect the general shape of the respective Franck–Condon transitions, with a slight preference of

population of higher vibrational states at larger scattering angles.

3.3.2. Molecular dication-atom

An early investigation of a single-electron non-dissociative transfer process, involving molecular dications, was

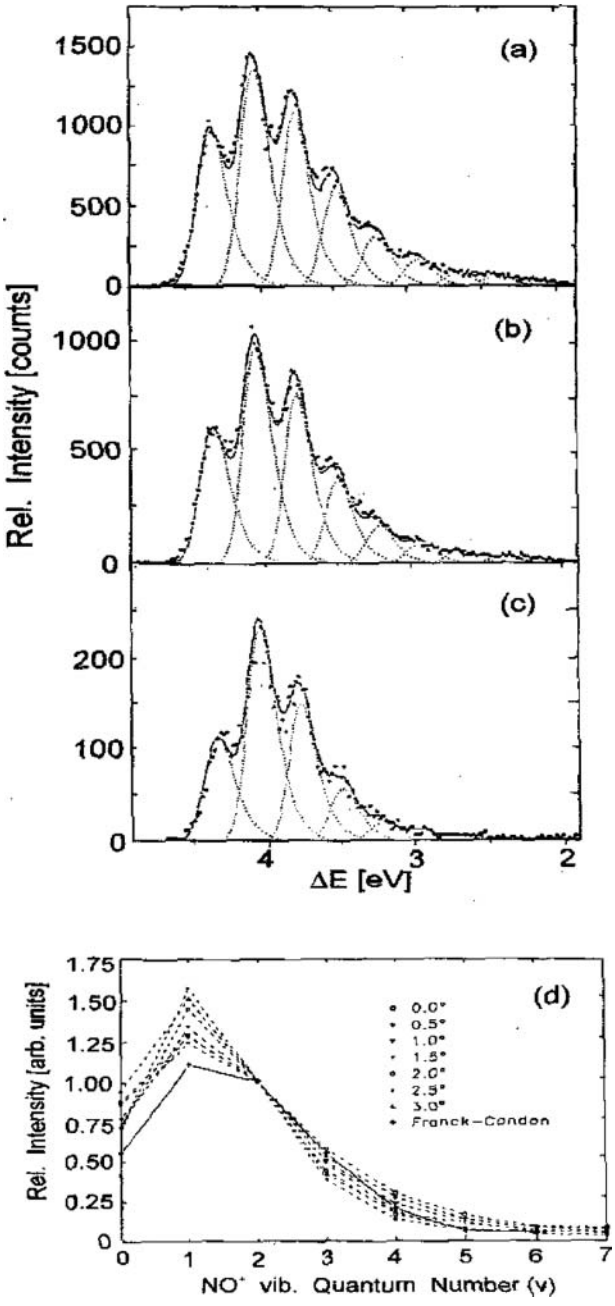

Figure 6. Translational energy spectrum of products $He^+ + NO^+$ from reaction (6) vs. reaction exothermicity ΔE at different scattering angles: (a) 0.0°; (b) 1.0°; (c) 2.5°; dashed lines – deconvolution of the spectra; (d) comparison of data with Franck–Condon factors as derived from photoelectron spectroscopy (solid line); dashed lines – deconvolution of the spectra.

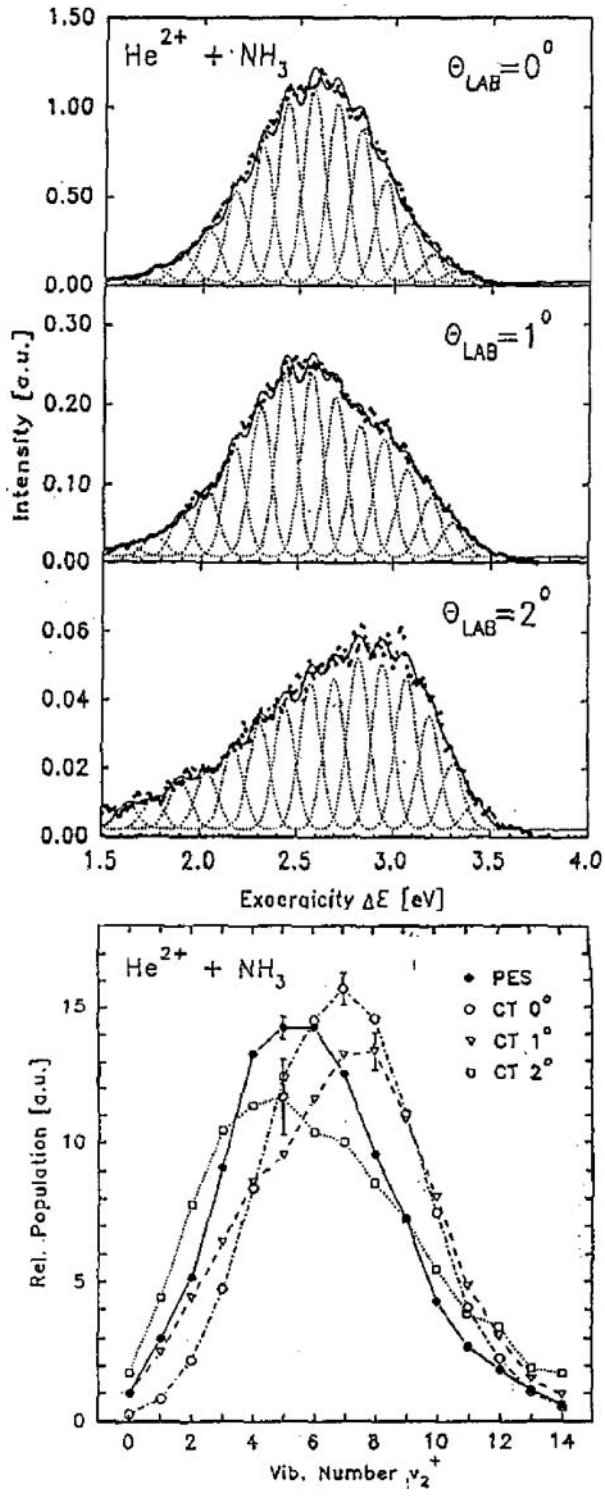

Figure 7. Translational energy spectrum of products $He^+ + NH_3^+$ from reaction (7) vs. reaction exothermicity ΔE at different scattering angles (a–c) and the respective deconvolution of the spectra; (d) comparison of the data with Franck–Condon factors as derived from photoelectron spectroscopy (solid line).

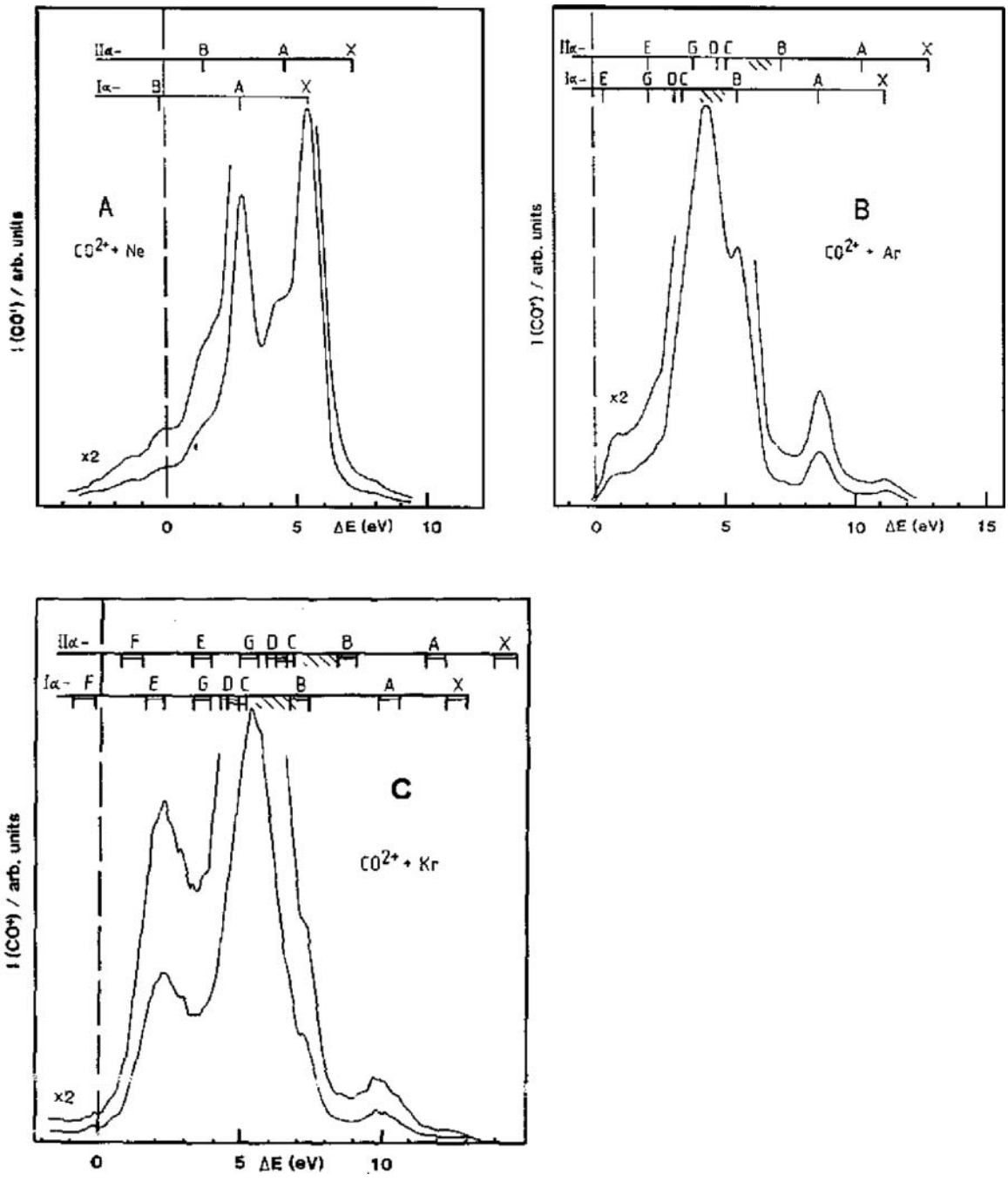

Figure 8. Translational energy spectra of CO^+ from reactions of 6 keV CO^{2+} with Ne (A), Ar (B) and Kr (C) vs. the reaction exothermicity ΔE. Scales refer to positions of the ground and excited states of CO^+; Iα refers to CO^{2+} ground state; IIα refers to the first excited state (placed as in the time of the experiment [14]).

translational energy spectroscopy using a tandem mass spectrometer carried out in 1986 [14]. Theoretical studies available at that time [27] gave some information on the molecular dication CO^{2+}, though even the ionisation energy of CO^{2+} was then not well known. Therefore, a study of non-dissociative single-electron transfer of this dication with noble gas atoms was undertaken [14]. The resolution at the rather high incident energy of the projectile diatomic dication of 6 keV was about 1 eV, thus, not allowing for distinguishing vibrational states of the internal states to be populated. Some of the results are given in Figure 8. At the time of the study, there was still a question about the spectroscopic assignment of the states of CO^{2+}. The study used the assignment of CO^{2+} ($^3\Pi$), confirmed correct later

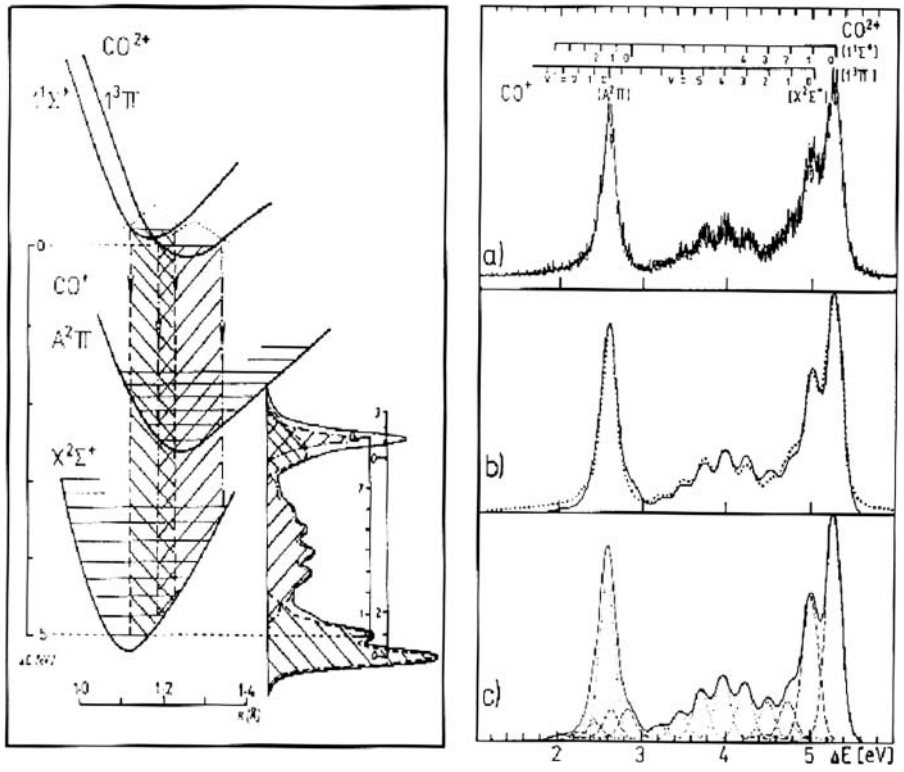

Figure 9. Analysis of the data on CO^{2+} + Ne of Hamdan and Brenton [28] by Fárník [29]. Left: potential energy curves and vertical transitions involved; right: comparison of experimental data (a) and calculations, (b) overall fit of experimental (solid line) and calculations (dotted), (c) same with individual transition probabilities (dashed).

on, as the lowest state, though the states lying above it were much in question (the position of the first excited state denoted in Figure 9 by IIα – using the Hasted's notation – had to be later corrected). Structures in the spectra suggested vibrational envelopes of the populated states of the product CO^+. However, the population of the electronic states formed was found to follow very well the reaction window concept: for CO^{2+} + Ne, the maximum was calculated to be located at 5.3 $\pm$ 1.1 eV, for CO^{2+} + Ar, at 4.4 $\pm$ 0.9 eV, and for CO^{2+} + Kr, at 4.1 $\pm$ 0.8 eV (the $\pm$ limits indicate the energy region with transition probability larger than 0.2).

The vibrational states of the product CO^+ were partly resolved shortly afterwards in a fine experiment of Hamdan and Brenton [28]. The published spectrum CO^{2+} + Ne at 6 keV was analysed later on by Fárník [29] in terms of vertical transitions between the potential energy curves of the molecular species of the system. At this high incident energy, the collision time is shorter than the vibrational period of the molecular species and thus, the inter-nuclear separation can be regarded as fixed during the transition. By then the position of the two lowest molecular states was well assigned [30], and it could also be concluded that – due to a low-lying dissociative state – the dications present in the beam were practically only in their ground vibrational states [29,31]. Four different transitions between the molecular species CO^{2+} and CO^+ contributed to the translational energy spectrum of CO^+ in reaction

$$\begin{aligned} &CO^{2+}(3\Pi,\ {}^1\Sigma^+;\ v=0) + Ne({}^1S_0) \\ &\quad \rightarrow CO^+(X^2\Sigma^+, A^2\Pi;\ v') + Ne^+({}^2P_j) \end{aligned} \qquad (8)$$

Population of the vibrational levels was determined from the overlap of the Franck–Condon factors of the respective transitions between of the electronic states of the molecular species, with relative cross sections of the electronic state-to-state processes, reflecting the (unknown) relative concentrations of the electronic states of CO^{2+} in the scattering centre, tentatively ascribed to achieve the fit. Figure 9 shows the excellent overall agreement between the experiment and the results of this analysis. Figure 9 is the summary of the analysis showing the potential curves used and the resulting calculated translational energy spectrum with the respective state-to-state contributions [29]. An analogous simulation analysis of reaction (8) was carried out for the results of a Prague low energy ($E_{LAB}(CO^{2+})$ = 7 eV) experiment [29]. The results of this analysis were in agreement with the experimental results, if the change

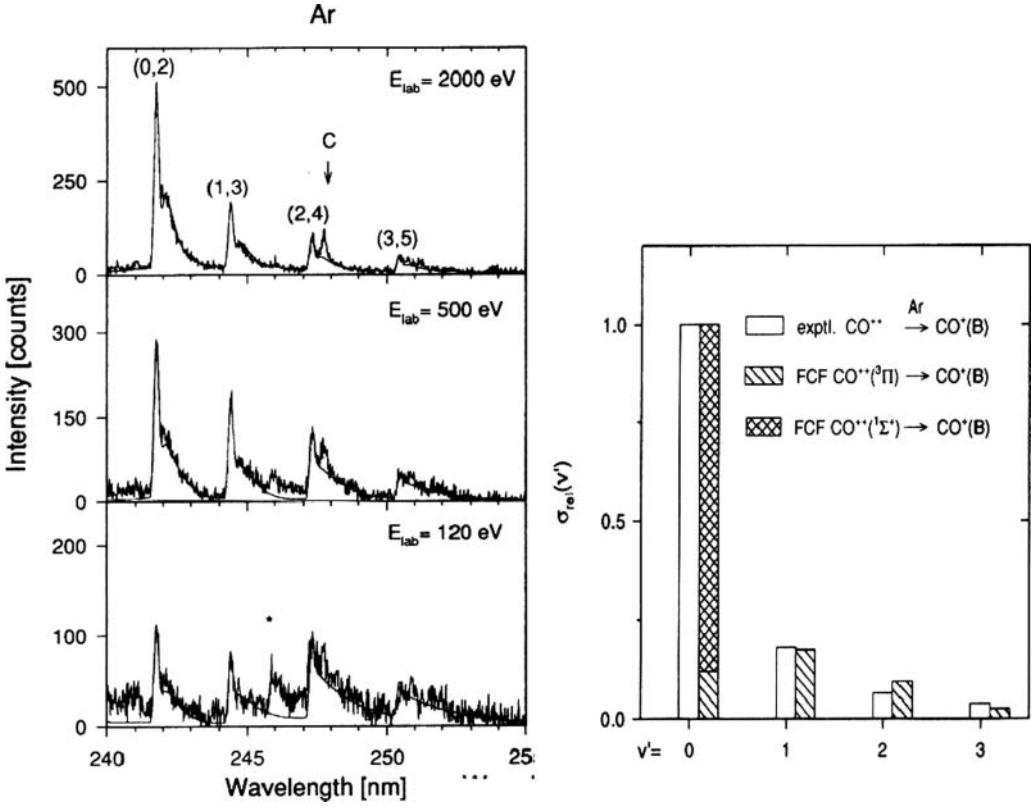

Figure 10. Left: sequence $\Delta v' = 2$ of the CO^+(B-X) emission spectra from reaction of CO^{2+} + Ar at three different energies of CO^{2+} – smooth line is the simulated spectral contour; right: relative cross sections for populations of the vibrational states v' at 2000 eV compared with distributions from Franck–Condon transitions, calculated for the two contributing states of the reactant CO^{2+} ($^3\Pi$, $v = 0$; $^1\Sigma^+$, $v = 0$).

of the inter-nuclear separation in this low-energy collision (collision time comparable to a vibrational period) was taken into consideration [5,29].

The results of the early study on the electron transfer process between CO^{2+} and Ar provided a motivation for a product luminescence study, in which emission of the reaction product CO^+ from the radiative excited state, formed in non-dissociative single-electron transfer between CO^{2+} and Ar, N_2, H_2, D_2 and CO, was investigated in collaboration with Ch. Ottinger group in Göttingen [16]. It followed from [14] that in CO^{2+} + Ar electron transfer collisions, the electronically excited state $CO^+(B^2\Sigma^+)$ was largely populated. Measuring its emission into the $CO^+(X^2\Sigma^+)$ ground state could therefore provide information on the population of vibrational and also, from the rotational envelopes of the vibrational transitions, rotational states of the molecular product ion in the reaction

$$CO^{2+}(^3\Pi,\ ^1\Sigma^+;\ v = 0) + Ar(^1S_0) \rightarrow CO^+(B^2\Sigma^+,\ v') + Ar^+(^2P_j) \qquad (9)$$

Figure 10 shows examples of the $CO^+(B^2\Sigma^+ \rightarrow X^2\Sigma^+)$ emission spectra from reaction (9) at different energies, and a comparison of the derived vibrational distributions of the product ion $CO^+(B^2\Sigma^+, v')$ with the calculated Franck–Condon transitions from the two reactant dications $CO^{2+}(^3\Pi, v = 0; ^1\Sigma^+; v = 0)$ into $CO^+(B^2\Sigma^+, v)$ [16]. Rotational temperature of the product, derived from the rotational envelopes of the vibrational peaks, was found for reaction (9) to be about 450–800 K, indicating formation of a rather cold molecular electron transfer product. The rotational temperature in CO^{2+} + N_2 was found even somewhat lower (about 400–500 K), corresponding practically to the temperature of the ionisation chamber [16].

3.3.3. *Molecular dication-molecule*

An even more interesting result came from investigation of the (B-X) emission from the following reaction [16]:

$$CO^{2+}(^3\Pi,\ ^1\Sigma^+;\ v = 0) + CO(X^1\Sigma^+) \rightarrow CO^+(B^2\Sigma^+,\ v') + CO^+(A^2\Pi,\ v'') \qquad (10)$$

Many internal states were involved in reaction (10) and thus a beam study in which the translational energy of the products would be measured was rather hopeless. In reaction (10) it was not obvious which product was formed

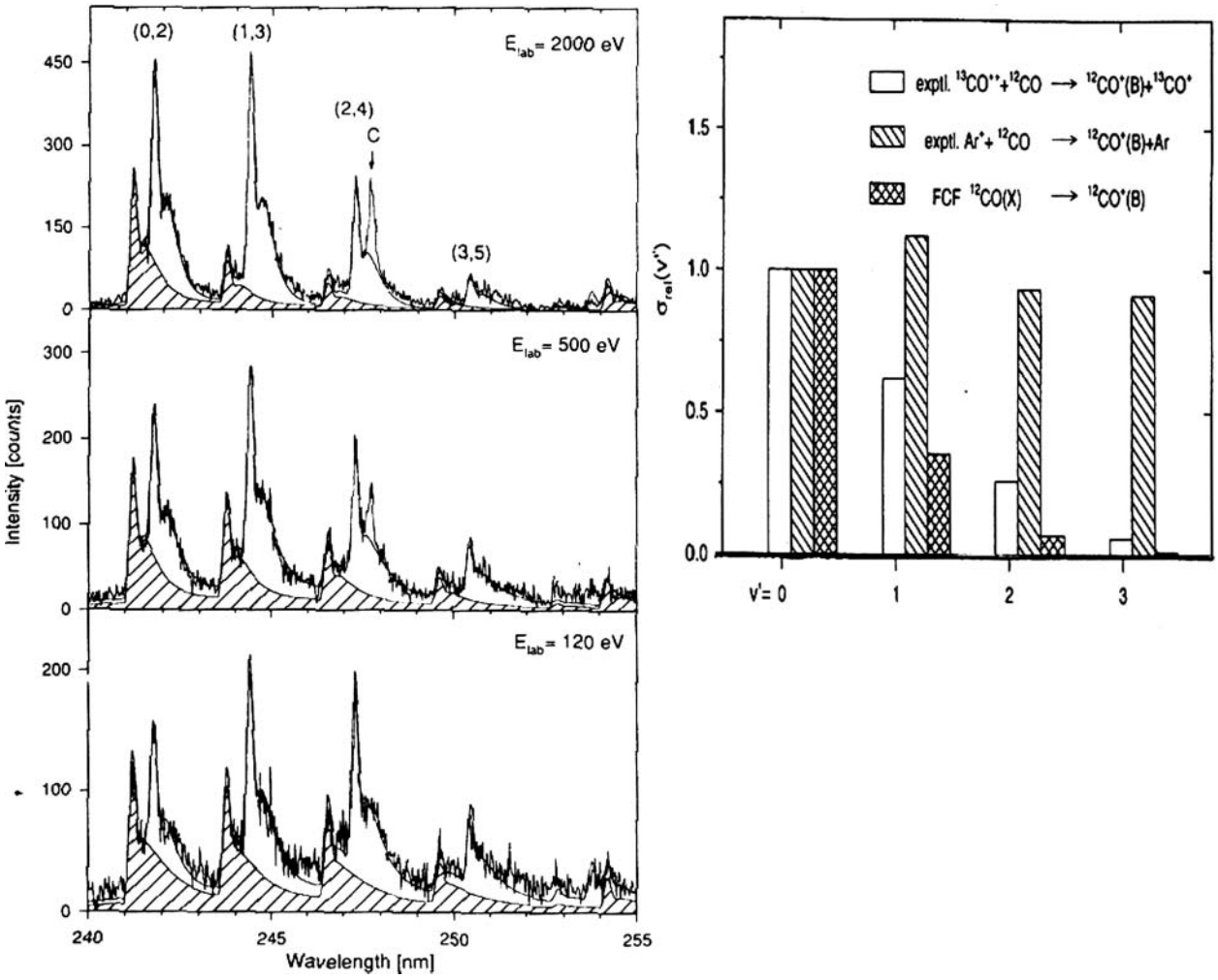

Figure 11. Left: CO^+(B-X) emission spectra from collisions of $^{13}CO^{2+}$ with ^{12}CO at three energies: the shaded portion is $^{13}CO^+$ emission from the electron capture by $^{13}CO^{2+}$; the rest is $^{12}CO^+$ emission from the ionised target; solid lines – simulated spectral contours. Right: comparison of the population of $^{12}CO^+$(B,v') states as obtained from the experiment (open columns) with populations derived from the respective Franck–Condon factors (hatched). For comparison, data on population of the $^{12}CO^+$(B,v') vibrational states, obtained from the cation–cation electron exchange reaction, $Ar^+ + CO \rightarrow Ar + CO^+$, are given to show an entirely different kind of process.

in the B and which in the A state and with what probability. Thus, it was found convenient to distinguish between the 'capture' process (formation of CO^+(B) from CO^{2+} by single-electron capture) and the 'ionisation' process (formation of CO^+(B) by ionisation of the neutral CO). The two processes were distinguished experimentally by using isotopically labelled $^{13}CO^{2+}$ projectile ions and ^{12}CO target molecules. The measured vibrational bands from capture and ionisation processes were then mutually isotopically shifted (Figure 11). First, it turned out that the branching ratio for CO^+(B), formed either by capture or ionisation, was about equal. Second and most important, the population of the vibrational states of CO^+(B) from the two processes differed: while those from the capture process were analogous to the results with Ar, N_2 and hydrogen, those from the ionisation process followed, at least approximately, the Franck–Condon factors of the transition CO(X)–CO^+(B) (Figure 11). [16].

The finding that the population of product internal states formed by the capture was different from that formed by the ionisation process was found useful in solving an even more complicated case of dissociative processes [31,32] in reaction

$$CO_2^{2+} + CO_2 \rightarrow CO^+ + O + CO_2^+ \qquad (11)$$

Using triple quadrupole and ion–ion coincidence mass spectrometry and appropriate isotope labelling (in order to distinguish the different reaction pathways), it was found that the primary CO_2^+ formed from the dication CO_2^{2+}

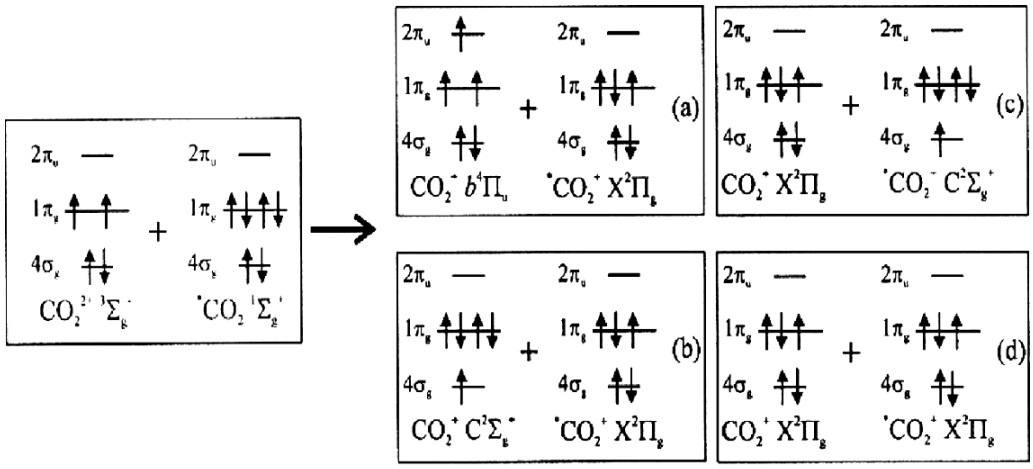

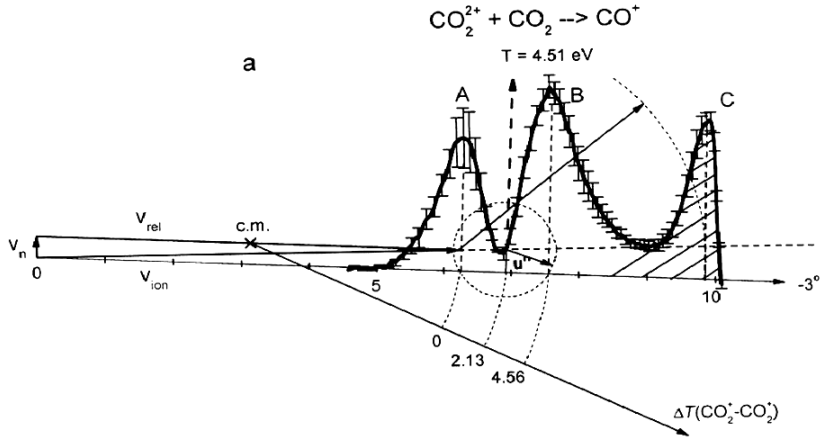

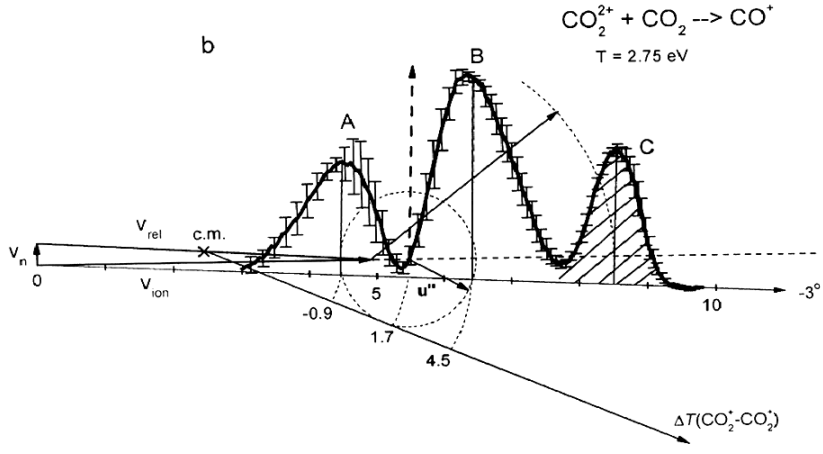

Figure 12. Dissociative electron transfer reaction (11), $CO_2^{2+} + CO_2 \rightarrow CO^+ + O + CO_2^+$. Upper part: schematics of the possible electronic states involved, indicating the one-electron transitions (more probable) and two-electron transitions (less probable). Lower part: velocity profiles of CO^+ from a crossed-beam experiment. The loci u'' on the circle indicate the relative velocity of CO^+ vs. O and originate at the position of the primary undissociated CO_2^+ formed (dashed vertical arrow) that slowly dissociates to CO^+ (peaks A and B relate to the forward and backward scattering of this product). Peak C comes from collision-induced dissociation of CO^{2+} on CO_2 and is not relevant to the present discussion of the electron transfer reaction.

(capture process) dissociates more readily than if formed from the neutral CO_2 (ionisation process, here, referred to as 'ejection' process) [31]. The case was rather complicated because of involvement of many states.

The basic reason is that the population of the key dissociative states of the primary electron transfer product, the CO_2^+ cation, is favoured by the CO_2^{2+} dication rather than by the neutral CO_2. Figure 12 (upper part) shows the relevant electronic configurations of different electronic states, leading to the dissociative process from the intermediate CO_2^+, formed both by the capture process from the dication and by the ionisation (ejection) process from the neutral molecule. Dissociative quartet states of CO_2^+ play crucial role in the formation of the dissociation products $CO_+ + O$. The quartet states are readily formed in a single-electron transition from the dication. On the other hand, the quartet states are far harder to populate from the neutral molecule, because this process requires a less probable two-electron transition [30,31].

Figure 12 shows the velocity profiles of the dissociation product CO^+ formed in the 'capture' process of reaction (11) [32]. Peaks A and B are the forward and backward wings of the dissociation product CO^+ from the dissociative electron transfer in CO_2^{2+}-CO_2 collisions (peak C comes from a different process, the collision-induced dissociation of CO^{2+} on CO_2, and is not important for this discussion). The data were interpreted as a subsequent slow dissociation of the primary reaction product CO_2^+ of a mean lifetime of at least several rotations, in agreement with the more detailed earlier data from coincidence experiments [31].

3.3.4. Conclusions: molecular systems

The data obtained for non-dissociative electron transfer in molecular systems showed that

(1) population of electronic states of the products follows the 'reaction window' concept also for molecular systems;
(2) population of vibrational states of products is very close to Franck–Condon transition factors of the respective vertical transitions between the dication-cation and neutral-cation states at high collision energies (collision time shorter than the vibrational period), at low collision energies small deviations occur (collision time comparable to the vibrational period);
(3) population of rotational states shows surprisingly rotationally cold reaction products: the rotational temperature of molecular product ions was found to be in most cases about 400–500 K, i.e. practically the temperature of the ion source.

Acknowledgements

This paper is dedicated to Břetislav Friedrich, a former colleague in J. Heyrovský Institute and co-author of the early papers mentioned in this communication, as an expression of my respect to his many contributions to various fields of chemical physics over the years.

The author wishes to express his thanks to the collaborators in the Prague Institute as mentioned in the references. The author would also like to offer special thanks to colleagues in the collaboration institutions, where some of the experiments were carried out (J.H. Beynon and his group at the Royal Society Research Unit, University College of Swansea, 1986; Max-Planck Institute für Strömunsforschung, Göttingen; J.P. Toennies and his group, 1990–1995; and Ch. Ottinger and his group, 1993–1996).

Financial support from the Royal Society Exchange Program – during the author's visit to Swansea – and from the Alexander von Humboldt Research Award (1992), which made the work in Göttingen possible, are gratefully acknowledged. Various parts of the research were supported by grants from the Grant Agency of the Czech Republic (203/93/0230; 203/00/0632) and the Grant Agency of the Academy of Sciences (440410; IAA 400400702).

References

[1] J.J. Thomson, *Rays of Positive Electricity* (Cambridge University Press, Cambridge, 1921), p. 84.
[2] A.L. Vaughan, Phys. Rev. **38**, 1687 (1931).
[3] R.K. Janev and H.-P. Winter, Phys. Rep. **117**, 265 (1985).
[4] D. Mathur, Phys. Rep. **225**, 193 (1993).
[5] Z. Herman, Int. Rev. Phys. Chem. **15**, 299 (1996).
[6] Z. Herman, Phys. Essays **13**, 480 (2000).
[7] Z. Herman, J. Žabka, Z. Dolejšek, and M. Fárník, Int. J. Mass Spectrom. **192**, 191 (1999).
[8] Z. Herman, Int. J. Mass Spectrom. **212**, 413 (2001).
[9] B. Friedrich and Z. Herman, Coll. Czech. Chem. Commun. **49**, 570 (1984).
[10] M. Fárník, Z. Herman, T. Ruhaltinger, J.P. Toennies, and R.G. Wang, Chem. Phys. Lett. **206**, 376 (1993).
[11] M. Fárník, Z. Herman, T. Ruhaltinger, and J.P. Toennies, J. Chem. Phys. **103**, 3495 (1995).
[12] W. Maring, J.P. Toennies, R.G. Wang, and H.B. Levene, Chem. Phys. Lett. **184**, 262 (1991).
[13] R.P. Morgan, J.H. Beynon, R.H. Bateman, and B.N. Green, Int. J. Mass Spectrom. Ion Phys. **28**, 171 (1978).
[14] Z. Herman, P. Jonathan, A.G. Brenton, and J.H. Beynon, Chem. Phys. Lett. **141**, 433 (1987).
[15] Ch. Ottinger and J. Simonis, Chem. Phys. **28**, 97 (1978).
[16] A. Ehbrecht, N. Mustafa, Ch. Ottinger, and Z. Herman, J. Chem. Phys. **105**, 9833 (1996).
[17] R.E. Olson and A. Salop, Phys. Rev. A **14**, 579 (1976).
[18] B. Friedrich, Š. Pick, L. Hládek, Z. Herman, E.E. Nikitin, A.I. Reznikov, and S.Ya. Umanskii, J. Chem. Phys. **84**, 807 (1986).
[19] B. Friedrich and Z. Herman, Chem. Phys. Lett. **107**, 375 (1984).
[20] J.P. Braga, D.B. Knowles, and J.N. Murrell, Mol. Phys. **57**, 665 (1986).
[21] B. Friedrich, J. Vančura, M. Sadílek, and Z. Herman, Chem. Phys. Lett. **120**, 243 (1985).
[22] B. Friedrich, J. Vančura, and Z. Herman, Int. J. Mass Spectrom. Ion Proc. **80**, 177 (1987).
[23] M. Sadílek, J. Vančura, M. Fárník, and Z. Herman, Int. J. Mass Spectrom. Ion Proc. **100**, 197 (1990).
[24] A. Dalgarno, Nucl. Instrum. Methods Phys. Res. B **9**, 655 (1985).

[25] R.W. Field, J. Mol. Spectrosc. **47**, 194 (1973).
[26] J.W. Rabalais, L. Karlsson, L.O. Werme, T. Bergmark, and K. Siegbahn, J. Chem. Phys. **58**, 3370 (1973).
[27] R.W. Wetmore, R.J. LeRoy, and R.K. Boyd, J. Phys. Chem. **88**, 6318 (1986).
[28] M. Hamdan and A.G. Brenton, J. Phys. B **22**, L45 (1989).
[29] M. Fárník, Ph. D. thesis, Charles University, Prague, 1991.
[30] M. Larsson, B.J. Olsson, and P. Sigray, Chem. Phys. **139**, 457 (1989).
[31] C.L. Ricketts, D. Schröder, J. Roithová, H. Schwarz, R. Thissen, O. Dutuit, J. Žabka, Z. Herman, and S.D. Price, Phys. Chem. Chem. Phys. **10**, 5135 (2008).
[32] J. Žabka, C.L. Ricketts, D. Schröder, J. Roithová, H. Schwarz, R. Thissen, O. Dutuit, S. D. Price, and Z. Herman, J. Phys. Chem. A **114**, 6463 (2010).